ELSEVIER

Int. J. Therm. Sci. 41 (2002) 241–252

International Journal of Thermal Sciences

www.elsevier.com/locate/ijts

Thermal transport phenomena over a slot-perforated flat surface in pulsating free stream

Shuichi Torii [a,*], Wen-Jei Yang [b]

[a] *Department of Mechanical Engineering, Kagoshima University, 1-21-40 Korimoto, Kagoshima 890-0065, Japan*
[b] *Mechanical Engineering and Applied Mechanics, University of Michigan, Ann Arbor, MI, 48109, USA*

Received 26 March 2000; accepted 11 March 2001

Abstract

A theoretical study is performed to investigate unsteady, two-dimensional, incompressible thermal-fluid flow over both sides of a slot-perforated flat surface, which is placed in a pulsating free stream. The effects of the pulsating Strouhal number, the Reynolds number *Re*, and the ratio of the slot width, d, to the plate thickness, δ, on the heat transfer performance and the velocity and thermal fields are disclosed. It is found from the study that: (i) when the free stream is pulsated, the alternating change in the fluid flow disturbs the thermal boundary layer formed along the plate and induces mixing of the upper and lower streams of the plate downstream from the slot, resulting in an amplification of heat-transfer performance; (ii) heat-transfer performance at the rear plate is induced with an increase in d/δ and *Re*; and (iii) heat transfer performance is intensified with an increase in fSr.

Keywords: Heat transfer; Perforated plate; Alternate crossing of flow; Numerical simulation; Pulsating Strouhal number

1. Introduction

In many compact heat exchanger applications, louver-fins, strip-fins, wavy-fins and perforated-fins are widely used to achieve high heat-transfer efficiency and compactness. A comparison of performances among these surfaces was made by Wong et al. [1]. The present study is focused on fluid flow and heat-transport phenomena over perforated plates placed in a free stream.

Perforated plates may be employed as an extended surface for internal cooling of turbine blades. They are compact and high in heat-transfer performance induced by boundary layer interruption due to perforations without the salient penalty of the form drag (Liang and Yang [2]; Liang et al. [3]; Lee and Yang [4]; Fujii et al. [5]; Hwang et al. [6]). Liang and Yang [7] investigated the flow characteristics and the mechanisms of plate vibration and noise, induced by the shedding of vortices from perforated holes. Furthermore, Liang [8] and Liang et al. [9] studied the effects of geometry and arrangement of the perforations on fluid flow behavior and disclosed that the ratio of slot length, in the flow direction, to its thickness plays a very important role in flow behavior. In order to investigate the effects of the Reynolds number and the ratio of the slot width, d, to the plate thickness, δ, on the velocity field, the corresponding numerical analysis was carried out by Torii and Yang [10,11]. They reported that the flow pattern between two plates placed in a free stream or two-dimensional channel can be classified into four categories depending on the combination of *Re* and d/δ. In particular, at a certain combination of *Re* and d/δ, an alternating crossing of flow of the fluid streams takes place through the slot from one side to the other side of the plate in the flow direction, so that the heat transfer performance from a surface wall of the rear plate was intensified (Torii et al. [12]). Amon and Mikic [13] performed numerical investigation of the flow pattern and forced convective heat transfer in slotted channels, in which numerical results are compared with the results with plane-channel flow. They disclosed that above a certain Reynolds number the flow exhibits laminar self-sustained oscillations, which cause significant heat transfer enhancement. Suzuki et al. [14] and Nigen and Amon [15] dealt with thermal fluid flow transport phenomenon in a plane channel with an in-line fin array and in a grooved channel, respectively. They reported that heat transfer performance is induced due to the self-sustained oscillatory flow.

* Correspondence and reprints.
E-mail addresses: torii@mech.kagoshima-u.ac.jp (S. Torii), wjyang@engin.umich.edu (W.-J. Yang).

1290-0729/02/$ – see front matter
PII: S1290-0729(01)01312-6

Nomenclature

B	calculation region	m
d	slot width	m
h	local heat transfer coefficient on the plate $= \frac{\lambda[\partial T/\partial y_w]}{T_w - T_{inlet}}$	$W{\cdot}m^{-2}{\cdot}K^{-1}$
L	length of plate	m
Nu	local Nusselt number $= h\delta/\lambda$	
$\overline{Nu}$	time-averaged Nusselt number on the plate	
P	pressure	Pa
Re	Reynolds number $= u_m\delta/\nu$	
fSr	pulsating Strouhal number $= \omega\delta/2\pi u_m$	
t	time	s
U, V	velocity components in streamwise and transverse directions, respectively, $U = u_m + u_b \sin\omega t$	$m{\cdot}s^{-1}$
u_b	amplitude of oscillating free-flow velocity	$m{\cdot}s^{-1}$
u_m	cycle-averaged velocity of pulsating free flow	$m{\cdot}s^{-1}$
x, y	coordinate	m
$\Delta X, \Delta Y$	mesh size	m
W	calculation region	m

Greek symbols

α	thermal diffusivity	$m^2{\cdot}s^{-1}$
ρ	density	$kg{\cdot}m^{-3}$
ν	molecular viscosity	$m^2{\cdot}s^{-1}$
δ	plate thickness	m
λ	thermal conductivity	$W{\cdot}m^{-1}{\cdot}K^{-1}$
θ	dimensionless temperature $= \frac{T - T_{inlet}}{T_w - T_{inlet}}$	
ω	angular frequency	$rad{\cdot}s^{-1}$
τ	dimensionless time $= t{\cdot}(2\pi{\cdot}\omega^{-1})$	

Subscripts

b	bulk
intel	intel
w	wall surface of the perforated plate

Unsteady flows are common in engineering applications. There is an enormous amount of literature on the subject of heat transfer in pulsating/oscillating channel and free-stream flows (for example, Bayler et al. [16]; Cooper et al. [17]; Dec et al. [18]; Feiler [19]; Jackson and Purdy [20]; Fujita and Tsubouchi [21]; Miller [27]). Studies on unsteady heat transfer under an external pulsation of flow have been reviewed by Gebhart et al. [22]. Ghaddar et al. [23,24] studied the effect of heat-transfer augmentation due to external pulsation at subcritical Reynolds numbers and discussed the mechanism of heat transfer enhancement inside a grooved channel under a pulsating flow. Greiner [25] carried out an experiment which supported the theory of Ghaddar et al. [23,24]. Azar [26] conducted an experimental investigation on the effect of forced oscillations on thermal transport in air entering a channel containing electronic circuitry. He reported that a critical groove frequency exists at which the cooling is maximized. These studies indicate that an external pulsation of flow induces amplification in heat transfer performance. As for thermal transport phenomena in a pulsating free-stream flow, Miller [27] investigated the effects of frequency and amplitude of oscillating flows on the local heat-transfer coefficient in the fully developed turbulent boundary layer over a flat plate. He concluded that the flow pulsation causes no heat transfer enhancement, whose behavior was also reported by Feiler [19]. In contrast, Fujita and Tsubouchi [21] conducted an experimental study on convective heat transfer from a uniformly heated flat plate in modulated flow and derived relationships for maximizing the heat-transfer augmentation due to the flow modulations. A similar heat-transfer argumentation due to the oscillatory and modulated flows is proposed by Cooper et al. [17]. Throughout the published results, we find no information on heat-transfer characteristics in the perforated plate placed in the oscillatory flow, i.e., the effect of a forced oscillations of the flow on heat-transfer enhancement due to the self-sustained oscillatory flow, i.e., an alternating crossing of flow of the fluid streams.

The present study investigates unsteady thermal and fluid flow transport phenomena over both sides of a slot-perforated surface, which is placed in a pulsating free stream. Emphasis is on the effects of pulsating Strouhal number, Reynolds number, and the ratio of the slot width, d, to the plate thickness, δ, on heat transfer performance and velocity and thermal fields. In this study the flow is assumed to be two-dimensional, to keep the computational time manageable. Three-dimensional computations, in general, will require extensive CPU times to conduct parametric tests such as those conducted here. Thus, the effect of three-dimensionality, which arises due to either secondary instabilities or end walls, is not taken into account.

2. Conservation equations and numerical procedure

The present study deals with a forced flow over a single-slot perforated surface heated with constant wall temperature in the pulsating free stream, which consists of two plain straight plates (i.e., the front and rear plates), of length, L, and thickness, δ, aligned in the flow direction with a spacing of d. Here two plates are set at $y = W/2$. Fig. 1 depicts the proposed physical model and the coordinate system. The following assumptions are imposed in the formulation of the problem: incompressible, laminar, unsteady flow;

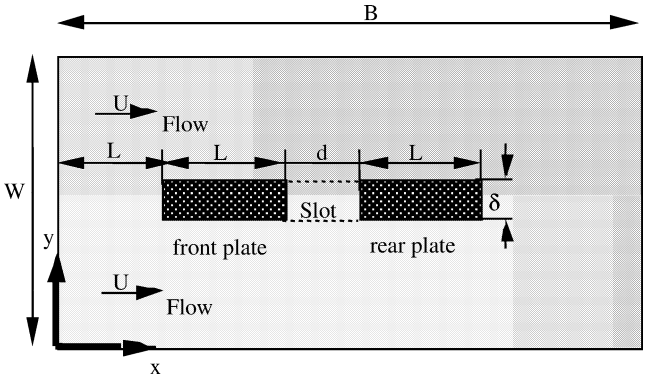

Fig. 1. A schematic of physical system and coordinate.

constant fluid properties; uniform inlet velocity and uniform inlet fluid temperature; and negligible axial conduction (due to the high Peclet number). Under these assumptions, the simplified governing equations for mass, momentum and energy read

$$\frac{\partial U}{\partial x}+\frac{\partial V}{\partial y}=0 \tag{1}$$

$$\frac{\partial U}{\partial t}+U\frac{\partial U}{\partial x}+V\frac{\partial U}{\partial y}=-\frac{\partial P}{\partial x}+\nu\left(\frac{\partial^2 U}{\partial x^2}+\frac{\partial^2 U}{\partial y^2}\right) \tag{2}$$

$$\frac{\partial V}{\partial t}+U\frac{\partial V}{\partial x}+V\frac{\partial V}{\partial y}=-\frac{\partial P}{\partial y}+\nu\left(\frac{\partial^2 V}{\partial x^2}+\frac{\partial^2 V}{\partial y^2}\right) \tag{3}$$

and

$$\frac{\partial T}{\partial t}+U\frac{\partial T}{\partial x}+V\frac{\partial T}{\partial y}=\alpha\left(\frac{\partial^2 T}{\partial x^2}+\frac{\partial^2 T}{\partial y^2}\right) \tag{4}$$

respectively. Note that P in Eqs. (2) and (3) includes ρ. Initially, the fluid is quiescent and at a uniform temperature at $T=T_{\text{inlet}}$. Then, the plate surface temperature is suddenly changed to $T=T_{\text{w}}$ and the free stream velocity is given at U $(=u_{\text{m}}+u_{\text{b}}\sin\omega t)$. Non-slip condition is employed at the plate surface. At the exit, the boundary conditions for the dependent variables are obtained by setting the first derivatives in the axial direction equal to zero. This is because the same use in other flow conditions is permissible for computational convenience if the outlet boundary is located in a flow region, which is sufficiently far downstream from the region of interest. Notice that the above boundary condition at the exit is strictly valid only when the flow is fully developed. As the boundary condition in the transverse direction, a free-stream condition is used, because the computational domain is sufficiently large, as mentioned in the following.

The discretization method employed in the present study uses a finite difference formulation and the discretized forms of the above governing equations read as:

$$U_{i,j}^{n+1}=U_{i,j}^{n}+\Delta t\left[\frac{1}{\Delta X}\left(P_{i,j}^{n}-P_{i+1,j}^{n}\right)-FUX^{n}-FUY^{n}+VISX^{n}\right] \tag{5}$$

$$V_{i,j}^{n+1}=V_{i,j}^{n}+\Delta t\left[\frac{1}{\Delta Y}\left(P_{i,j}^{n}-P_{i,j+1}^{n}\right)-FVX^{n}-FVY^{n}+VISY^{n}\right] \tag{6}$$

$$T_{i,j}^{n+1}=T_{i,j}^{n}+\Delta t\left[-FTX^{n}-FTY^{n}+VIST^{n}\right] \tag{7}$$

The subscript and superscript correspond to the cell location and time level, respectively. A detailed description of the above discretization method and FUX^n, FUY^n, $VISX^n$, FVX^n, FVY^n, and $VISY^n$ in Eqs. (5) and (6), are available in the literature (Harlow and Welch [28]; Hirt et al. [29]) and thus are not repeated here. FTX^n, FTY^n, and $VIST^n$ in Eq. (7) are also expressed in the literature (Torii and Yang [10,11]). The system variables P, U, V and T are calculated with a staggered grid proposed by Harlow and Welch [28]. The processes involved in completing one calculation cycle at an arbitrary time-step are as follows: (i) by solving Eqs. (5)–(7) for U, V and T, subject to the appropriate boundary conditions, the new velocities, which involve the values for the contributing pressure and velocities at the previous time-step, are predicted for the entire mesh to be solved; (ii) these velocities are iteratively adjusted to satisfy the continuity equation, Eq. (1), by making appropriate changes in the cell pressures, that is, each cell in the iteration is considered successively and is given a pressure change that drives its instantaneous velocity divergence to zero (Torii et al. [12]); (iii) when convergence has been reached with a maximum relative change in the values between successive iterations of less 10^{-4}, the velocity and pressure fields are determined at the advanced time level and are used as starting values at next time-step. These processes are repeated until t reaches a prescribed time, say, $t=80$ s after the calculation is initiated. Note that at this time, the thermal transport phenomenon becomes periodic, that is, a steady time-periodic solution is obtained, as shown in the following.

The grid system is changed from 200×400 to 400×800 to obtain a grid-independent solution and to confirm the fully developed and free-stream conditions mentioned above. Hence, a grid system of 200×400 ($W\times B$) nodal points with uniformly distributed nodal points, whose domain corresponds to $W/\delta=20$ and $B/\delta=40$, is employed to save computation time. When the pre-calculation was performed using the domain with $W/\delta=60$ and $B/\delta=120$, the first derivatives in the transverse and streamwise directions were almost zero over the flow field, i.e., $W/\delta>20$ and $B/\delta>40$, respectively. In other words, the corresponding flow region is not affected by the presence of the perforated plate. Thus, this implies that the free-stream and fully-developed conditions are satisfied as mentioned above. Numerical computation was performed on a personal computer (Pentium II CPU 266 MHz) at time interval $\Delta t=0.00001$ s, which consumed up to 24 CPU hours, using air as the working fluid ($Pr=0.71$). Here, the maximum time interval employed is determined to ensure the numerical stability. Based on the dataset obtained here, visualization of

the flow and thermal fields is carried out using a commercially available 2-D graphics software tool.

In general, time-mean heat transport phenomenon in a pulsating flow is affected by five dimensionless parameters, i.e., Re $(= u_m\delta/\nu)$, fSr $(= \omega\delta/2\pi u_m)$, Pr, u_b/u_m, $u_m/\omega\delta$. Here, although the last parameter is important for the transport phenomenon, in the pulsating flow with the long wavelength its parameter is correlated as $u_m/(\omega\delta) = 1/(2\pi fSr)$ using fSr. In the present study, $u_b/u_m = 0.20$ is fixed because the effect of pulsation amplitude on heat-transfer enhancement is not considered. L/δ are fixed at 2, while the Reynolds number (Re) is varied from 100–1100, d/δ is varied from 2.0 to 4.0, and pulsating Strouhal number, fSr, is varied from 0–10.

Simulations with grids of various degrees of coarseness, as mentioned earlier, were conducted to determine the required resolution for grid-independent solutions. Throughout the Reynolds number range considered here, the maximum error was estimated to be about 2% by comparing the solutions on regular and fine grids with twice the grid points. The calculated temperature field is directly affected by the accuracy of the predicted velocity one, because the temperature is obtained from the energy equation using the predicted velocity. Moreover, since the heat transfer coefficient is related to the temperature gradient in the vicinity of the heated plate, as shown in nomenclature, the Nusselt number is affected by the accuracy of the predicted temperature and velocity fields. In the prediction, the difference of the average Nusselt number on the plate between on regular and fine grids with twice the grid points was less than 2%. Although a few solutions were computed with half the time step to ensure consistency and time-step independence, there was no substantial discrepancy between two different time intervals.

3. Results and discussion

The structure of the flow over the single-slot perforated plate and the wake of the rear plate are discussed through the use of computed instantaneous velocity vectors. Fig. 2, for $Re = 120$ and $\tau = 0$ s, depicts the instantaneous maps of fluctuating velocity vector for the different pulsating free streams, fSr and the dimensionless slot-width, d/δ. Notice that velocity components are normalized by dividing by inlet velocity and the computational domain of $20\delta(= x) \times 5\delta(= y)$ is depicted in figures and the dimensionless time $\tau = 0$ in the figures corresponds to $t = 120$ s. Fig. 2(a)–(d) show the numerical results at $fSr = 0$ and $d/\delta = 2.0$, $fSr = 10$ and $d/\delta = 2.0$, $fSr = 0$ and $d/\delta = 4.0$, and $fSr = 10$ and $d/\delta = 4.0$, respectively. Here, the phase angle of the applied forcing, ωt, is π in Fig. 2(b) and (d). The corresponding temperature distributions, i.e., isotherms, are illustrated in Fig. 3, in which $\theta = 1$ and 0 correspond to the heated-plate temperature and the fluid temperature in free stream, respectively. It is observed in Figs. 2(a) and 3(a) that (i) the fluid flows straight downstream and a recirculation zone occurs at the wake region of each plate with the flow dipping into the slot from both sides, and (ii) the streamwise development of the thermal boundary layer is somewhat disturbed due to the presence of this recirculation zone. One observes in Fig. 2(b) that mixing of the upper and lower streams of the plate downstream from the slot is enhanced by the presence of the pulsating free stream. An increase in slot width induces the alternating change in the flow direction across the slot, resulting in amplification of the thermal diffusion from the plate along the flow, as shown in Figs. 2(c) and 3(c). This change is enhanced by the presence of the pulsation of the free stream, as seen in Figs. 2(d) and 3(d). In other words, the alternating change in the flow direction across the slot yields an increase in thermal diffusion from the rear plate, which is induced due to the pulsating free stream. It is expected, therefore, that the flow characteristic, i.e., the alternating change in the flow direction, has an effect on heat transfer from the rear plate.

Fig. 8, for $Re = 120$, illustrates the time records of the Nusselt number, Nu, at one side wall of the rear plate. Note that since there is no appropriate time scale for $fSr = 0$, the dimensionless time τ is determined using the time scale at $fSr = 10$. Since the thermal transport phenomenon, from the calculation results, becomes periodic after about $t =$ 80 s, numerical results during arbitrary time interval, i.e., of $t = 100$ s to $t = 110$ s are shown in Fig. 8. Here, Nu implies the averaged Nusselt number over one side wall of the plate at each dimensionless time, τ, which is normalized by the time scale, i.e., the cycle period ωt from 0 to 2π and $\tau = 0$ corresponds to $t = 100$ s. The Nusselt number at $d/\delta = 2$ is always constant as time progresses and this level is slightly increased with an increase in fSr. This is because the flow and temperature patterns in Figs. 2(a) and 3(a) remain steady, as evidenced by the absence of temporal variation in both the velocity vector and the isotherm, resulting in no periodic variation of heat transfer from the rear plate and a little dynamic behavior due to the pulsation of the free stream is linked to the use of small u_b/u_m, i.e., $u_b/u_m = 0.2$. By contrast, the heat transfer rate at $d/\delta =$ 4 oscillates with time and is substantially enhanced. This trend is induced by the presence of the pulsation of the free stream, i.e., $fSr = 10$. The oscillation of the heat transfer rate with time is caused by the alternating changes in the fluid flow across the slot. The heat transfer enhancement becomes clearer for the timewise variation of flow patterns and isotherms over both sides of the single-slot perforated plate. Fig. 4, for $d/\delta = 4$, depicts a sequence of alternating crossing of fluid flow from one side of the plate to the other through the slot in the absence of the pulsating free stream. The corresponding isotherm patterns are illustrated in Fig. 5. Consecutive images in Figs. 4 and 5 are obtained at a dimensionless time interval of 5.0. The alternating change in the flow direction across the slot induces thermal diffusion from the plates along the flow, as shown in Fig. 5. This results in a regular change in temperature distributions in the flow direction, particularly behind the rear plate. This change

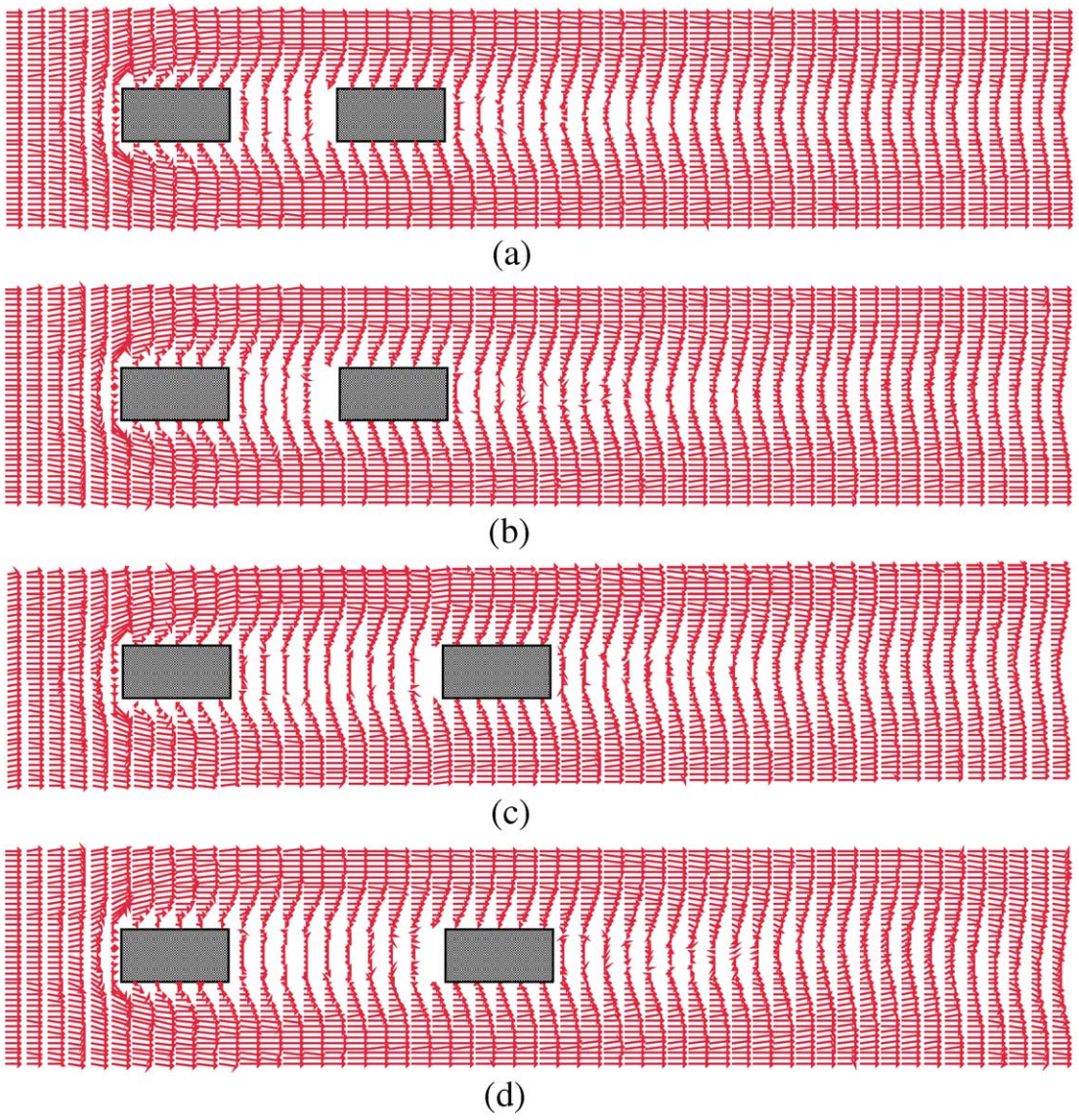

Fig. 2. Instantaneous maps of velocity-vector field around the perforated plate for $Re = 120$ and $\tau = 0$ s: (a) $d/\delta = 2.0$, $fSr = 0$; (b) $d/\delta = 2.0$, $fSr = 10$; (c) $d/\delta = 4.0$, $fSr = 0$; (d) $d/\delta = 4.0$, $fSr = 10$.

is induced by the presence of the pulsation of the free stream, as seen in Figs. 6 and 7. Figs. 6 and 7 illustrate numerical results at $fSr = 10$ and $d/\delta = 4.0$ and show the timewise variation of flow and isotherm patterns over both sides of the single-slot perforated plate, respectively. As time progresses, the regular changes in temperature and velocity distributions behind the rear plate are enhanced beyond the corresponding one at $fSr = 0$ and $d/\delta = 4.0$. The higher heat-transfer rate at the rear plate is achieved for $d/\delta = 4$ than for $d/\delta = 2$; that is, the amplification of the Nusselt number is caused by an increase in slot width. In other words, the alternating changes in the fluid flow result in an amplification of the heat transfer performance at the rear wall. This amplification becomes greater due to the presence of the pulsation of the free stream.

Fig. 9, for a fixed $fSr = 0$, compares the time-averaged Nusselt number, $\overline{Nu}$, on the rear plate wall against the Reynolds number with different d/δ. The Nusselt number is increased with an increase in the Reynolds number as expected. Higher heat-transfer performance yields at $d/\delta = 4.0$ over the wide range of the Reynolds number. It is found that at the same Reynolds number, an increase in the slot width induces the alternating changes in the fluid flow, resulting in an amplification of the heat-transfer performance at the rear wall.

The effect of the pulsation of the free stream on the time-averaged Nusselt number is illustrated in Fig. 10, in the same form as Fig. 9, in which d/δ is fixed at 4.0. The Nusselt number is intensified with increasing pulsation of the free stream, i.e., fSr. This trend becomes greater in the higher Reynolds number region plotted. In other words, the

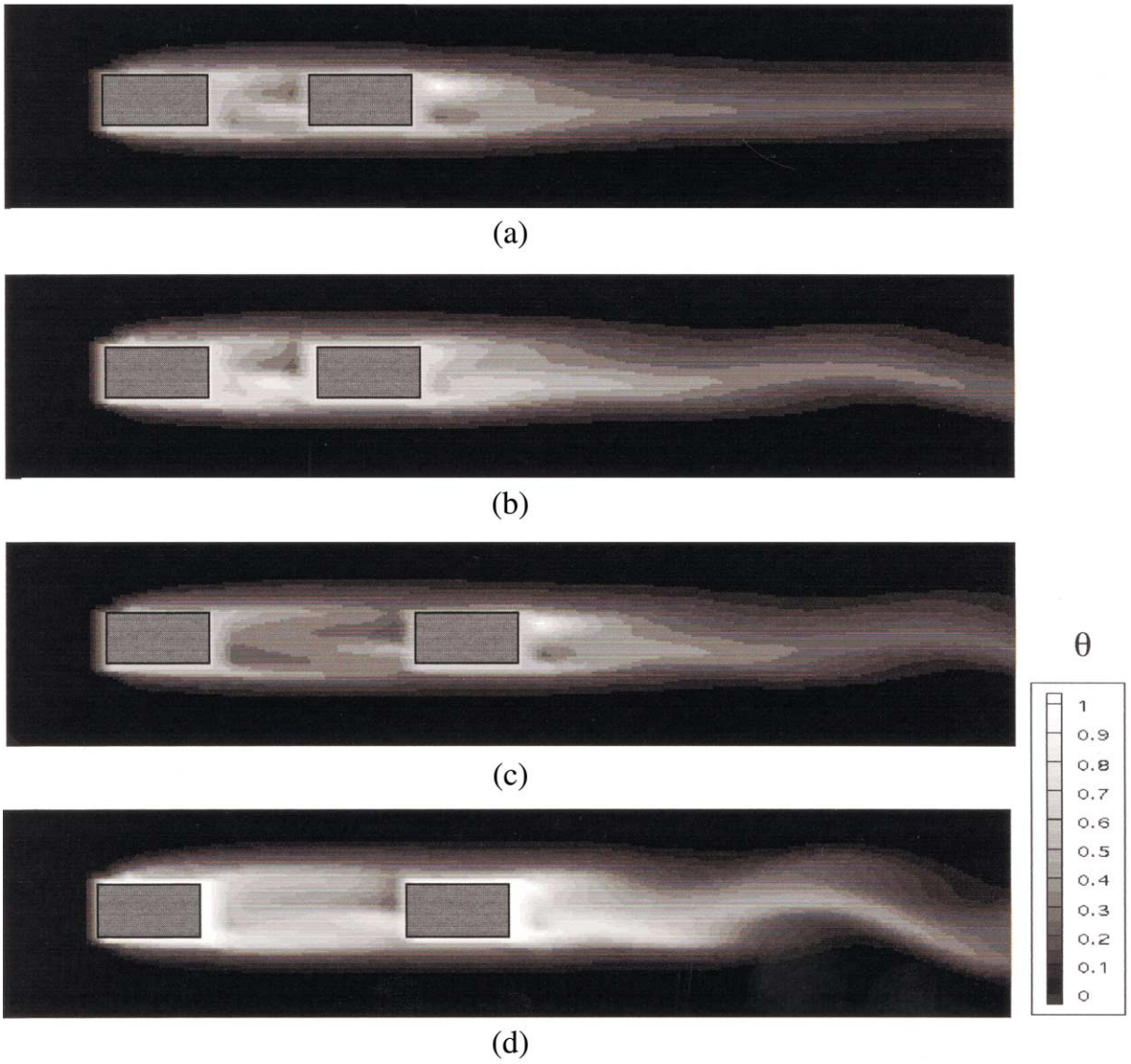

Fig. 3. Instantaneous maps of temperature field around the perforated plate for $Re = 120$ and $\tau = 0$ s: (a) $d/\delta = 2.0$, $fSr = 0$; (b) $d/\delta = 2.0$, $fSr = 10$; (c) $d/\delta = 4.0$, $fSr = 0$; (d) $d/\delta = 4.0$, $fSr = 10$.

effect of the pulsation frequency of the free stream on an enhancement of heat-transfer performance becomes minor in the lower Reynolds number region. Notice that when the value of fSr increases substantially over 10, heat transfer is uniformly enhanced over the Reynolds number region plotted.

4. Summary

A numerical study has been performed on unsteady thermal-fluid flow over a perforated plate (consisting of two plates spaced at an interval of d in the flow direction) installed in a pulsating free stream. Consideration was given to the roles of the Reynolds number, the pulsating Strouhal number, and the ratio of the slot width, d, to the plate thickness, δ, on the flow and temperature fields. It was found that:

(1) An increase in d/δ induces alternating changes in the fluid flow, resulting in an amplification of the heat-transfer performance at the rear wall.
(2) When the free stream is pulsated, the alternating change in the fluid flow induces an amplification of the heat-transfer performance at the rear wall of the rear plate.
(3) Heat-transfer performance is intensified with an increase in fSr.

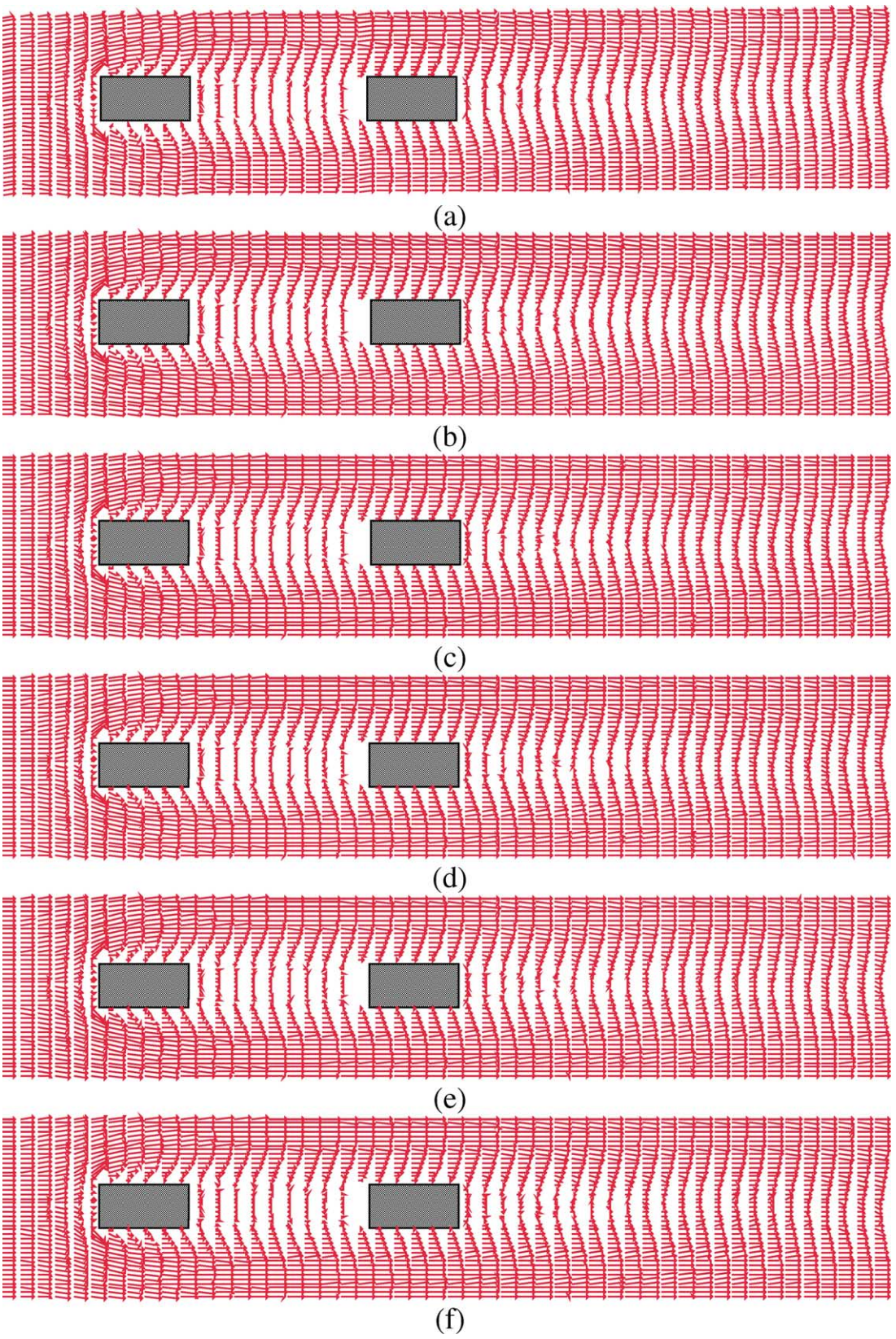

Fig. 4. Timewise variation of velocity-vector field around the perforated plate at a dimensionless time interval of $\tau = 5.0$, for $Re = 120$, $d/\delta = 4.0$, $fSr = 0$.

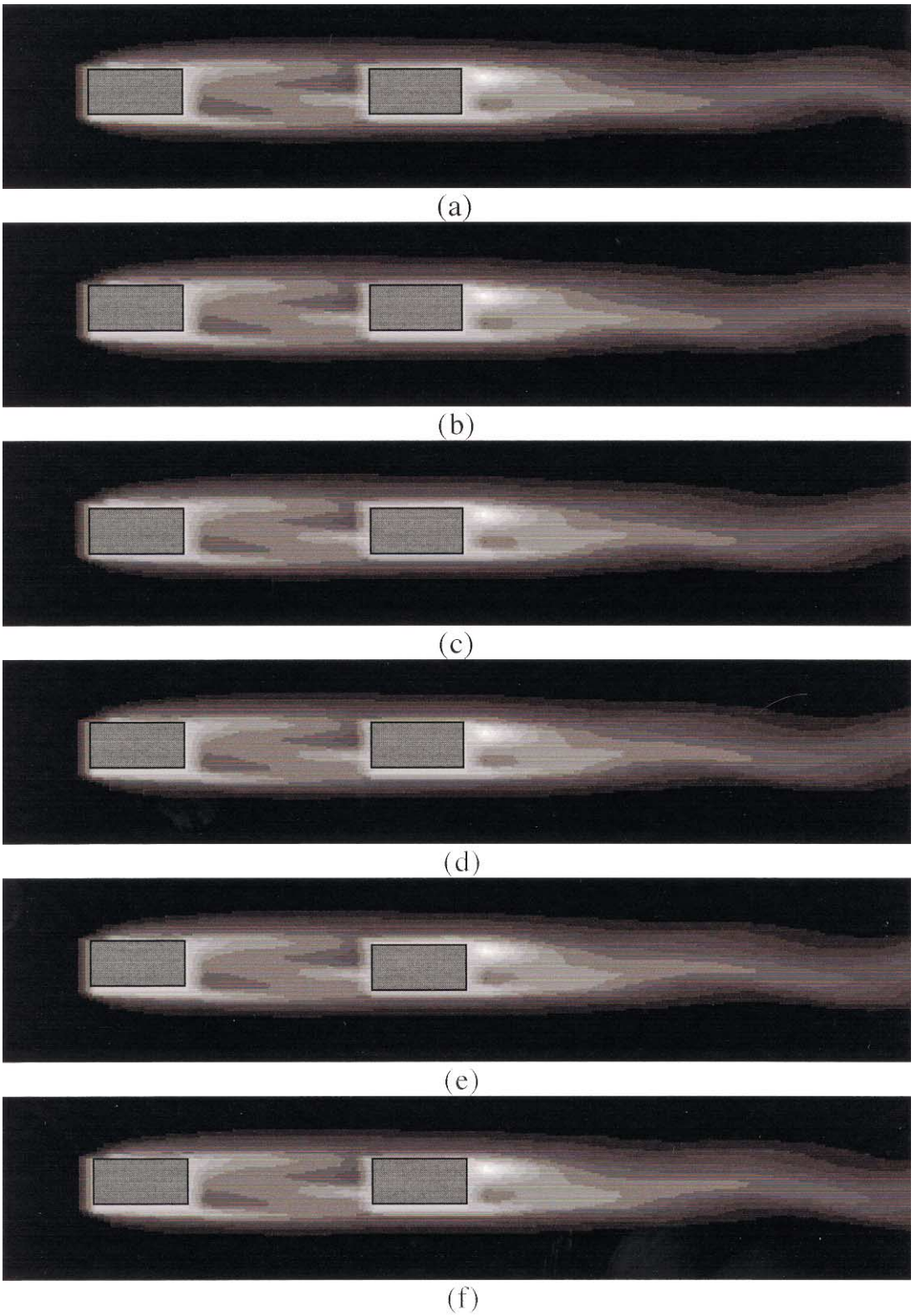

Fig. 5. Timewise variation of temperature field around the perforated plate at a dimensionless time interval of $\tau = 5.0$, for $Re = 120$, $d/\delta = 4.0$, $fSr = 0$.

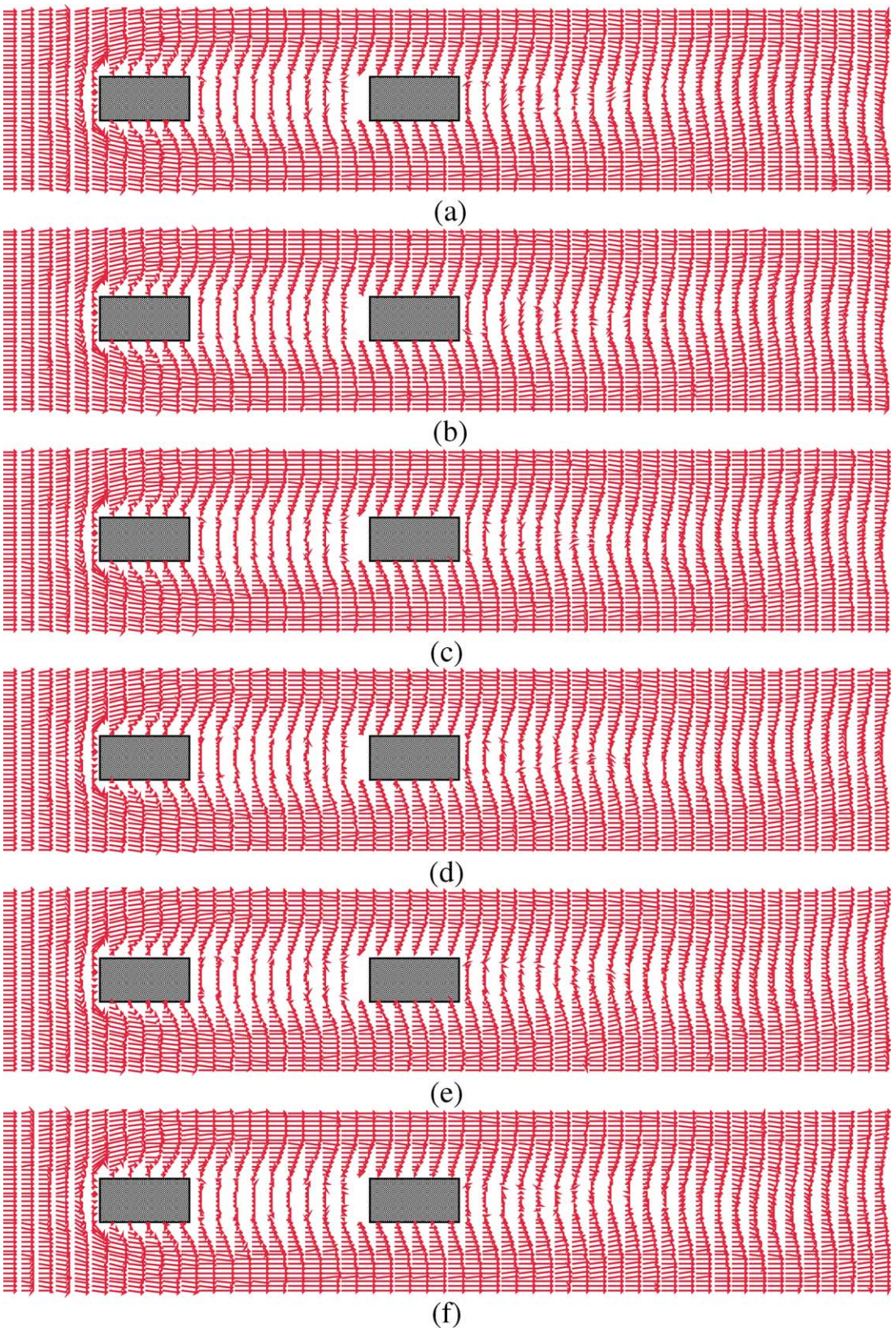

Fig. 6. Timewise variation of velocity-vector field around the perforated plate at a dimensionless time interval of $\tau = 5.0$, for $Re = 120$, $d/\delta = 4.0$, $fSr = 10$.

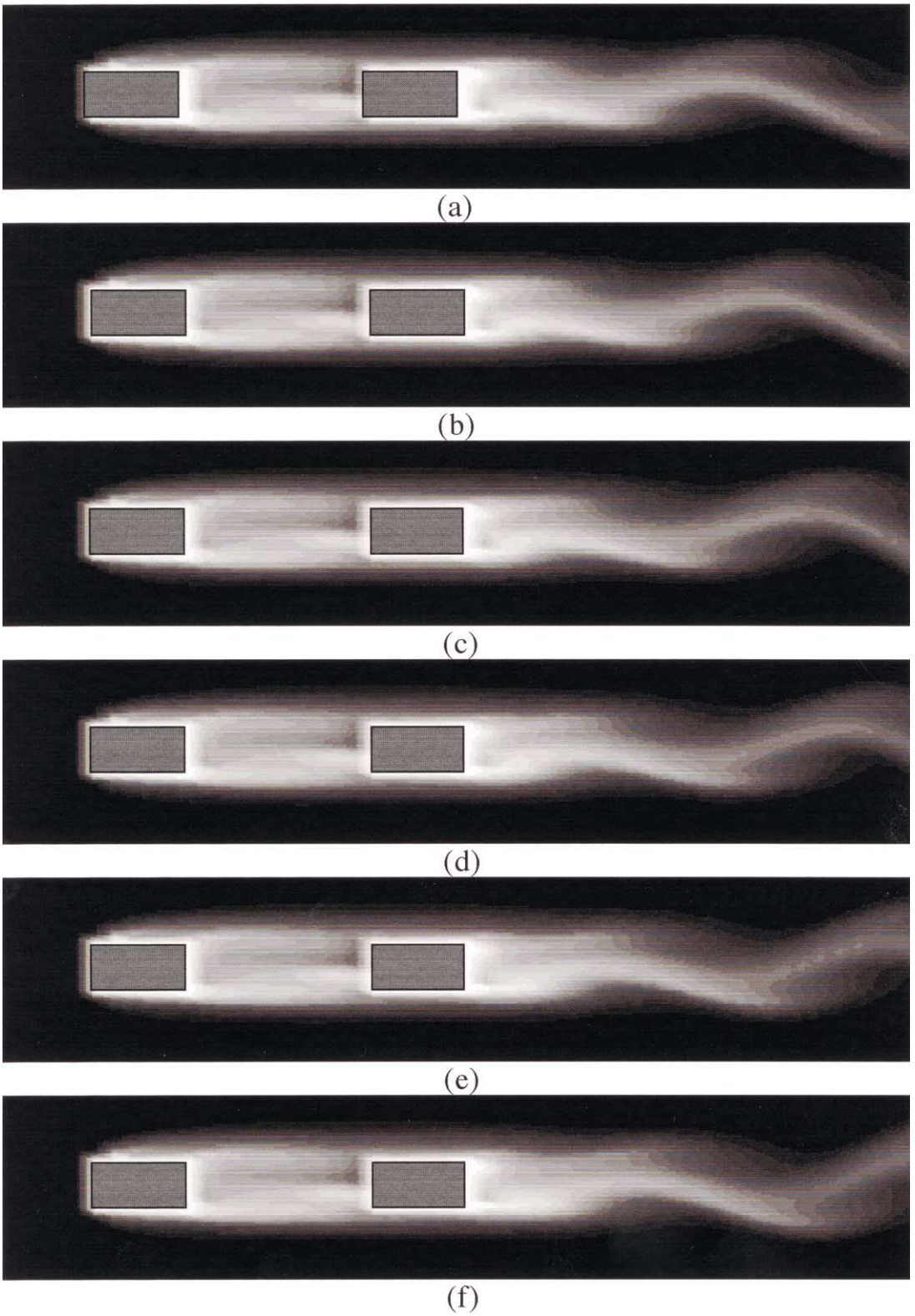

Fig. 7. Timewise variation of temperature field around the perforated plate at a dimensionless time interval of $\tau = 5.0$, for $Re = 120$, $d/\delta = 4.0$, $fSr = 10$.

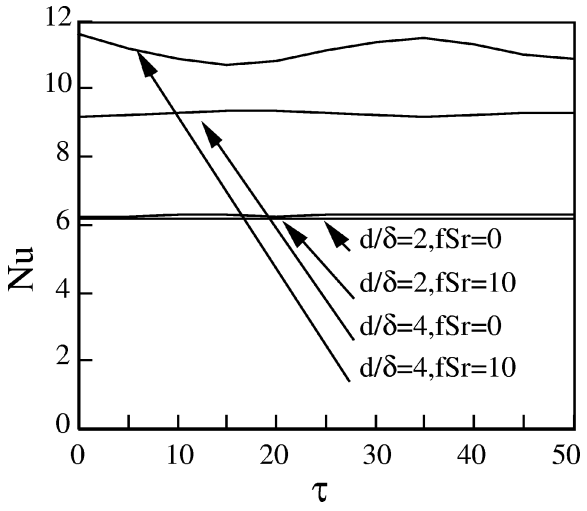

Fig. 8. Timewise variation of Nusselt numbers at rear plate for $Re = 120$.

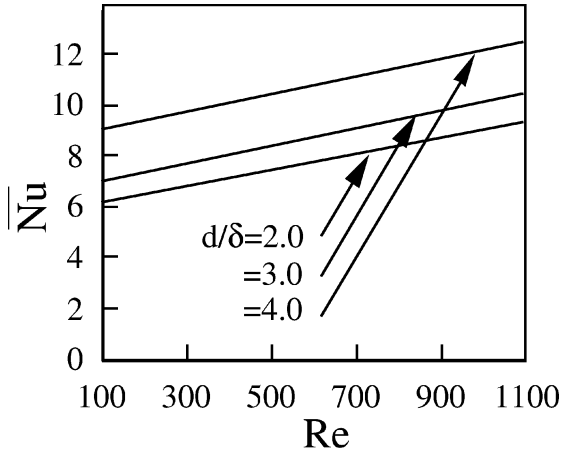

Fig. 9. Time-averaged Nusselt numbers for different slot width for $fSr = 0$.

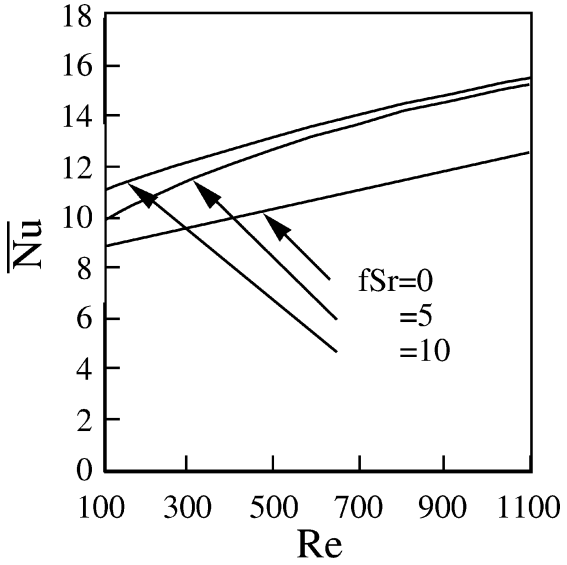

Fig. 10. Time-averaged Nusselt numbers for different pulsating Strouhal numbers, fSr, for $d/\delta = 4$.

References

[1] S. Wong, J.D. Duncan, J.C. Gibson, J.J. Killackey, Compact condenser for rankine cycle engine, Final Report 71-7464, (Prepared for Environmental Protection Agency), Air Research Manufacturing Co., CA, 1971.

[2] C.Y. Liang, W.-J. Yang, Heat transfer and friction loss performance of perforated heat exchanger surface, ASME Heat Transfer Conf. 97 (1975) 9–15;
C.Y. Liang, W.-J. Yang, Modified single blow technique for performance evaluation on heat transfer surface, ASME Heat Transfer Conf. 97 (1975) 16–21.

[3] C.Y. Liang, W.-J. Yang, Y.Y. Hung, Perforated-fin type compact heat exchangers for gas turbines, in: Tokyo Joint Gas Turbine Congress, 1977, pp. 77–85.

[4] C.P. Lee, W.-J. Yang, Augmentation of convective heat transfer from high-porosity perforated surfaces, Heat Mass Transfer 1978-Toronto 2 (1978) 589–594.

[5] M. Fujii, S. Seshimo, G. Yamanaka, Heat transfer and pressure drop of perforated surface heat exchanger with passage enlargement and contraction, Internat. J. Heat Mass Transfer 31 (1) (1988) 135–142.

[6] G.J. Hwang, C.C. Wu, L.C. Lin, W.-J. Yang, Investigation of flow drag and forced convective heat transfer in perforated coolant channels, in: Transport Phenomena in Combustion, Vol. 2, Taylor and Francis, 1996, pp. 1747–1758.

[7] C.Y. Liang, W.-J. Yang, Frequency of vortex shedding, vibration and noise in perforated-plate stacks, in: Proc. 12th Annual Meeting of Soc. of Engrg. Sci., 1975, pp. 797–806.

[8] C.Y. Liang, Heat transfer, flow friction, noise and vibration studies of perforated surface, Ph.D. Thesis, University of Michigan, Ann Arbor, MI, 1975.

[9] C.Y. Liang, C.P. Lee, W.-J. Yang, Visualization of fluid flow past perforated surfaces, in: Proc. Japanese 4th Symp. Flow Visualization, 1976, pp. 69–73.

[10] S. Torii, W.-J. Yang, Numerical flow visualization of a slot-perforated flat surface in free stream, 1998-CSME 1 (1998) 177–184.

[11] S. Torii, W.-J. Yang, Flow over a slot-perforated flat surface between two parallel plates, in: Proceedings of 8th International Symposium of Flow Visualization, No. 006, 1998, pp. 1–8.

[12] S. Torii, W.-J. Yang, S. Umeda, Flow visualization and transport phenomena over a slot-perforated flat surface between two parallel plates, J. Flow Visualization and Image Processing 5 (1998) 63–80.

[13] C.H. Amon, B.B. Mikic, Spectral element simulations of unsteady forced convective heat transfer: application to compact heat exchanger geometries, Numer. Heat Transfer A 19 (1991) 1–19.

[14] K. Suzuki, G.N. Xi, K. Inaoka, Y. Hagiwara, Mechanism of heat transfer enhancement due to self-sustained oscillation for in-line fin array, Internat. J. Heat Mass Transfer 37 (1994) 83–96.

[15] J.S. Nigen, C.H. Amon, Time-dependent conjugate heat transfer characteristics of self-sustained oscillatory flows in a grooved channel, J. Fluid Engrg. 116 (1994) 499–507.

[16] F.J. Bayler, P.A. Edwards, P.P. Singh, The effect of flow pulsations on heat transfer by forced convection from a flat plate, in: Proceedings of the First International Heat Transfer Conference, Boulder, CO, 1961, pp. 499–509.

[17] W.L. Cooper, V.W. Nee, K.T. Yang, An experimental investigation of convective heat transfer from the heated floor of a rectangular duct to a low frequency, large tidal displacement oscillatory flow, Internat. J. Heat Mass Transfer 37 (1994) 581–592.

[18] J.E. Dec, J.O. Keller, V.S. Arpaci, Heat transfer enhancement in the oscillating turbulent flow of a pulsed combustor tail pipe, Internat. J. Heat Mass Transfer 37 (1992) 2311–2325.

[19] C.E. Feiler, Experimental heat transfer and boundary layer behavior with 100-CPS oscillations, NASA TN No. 2531, 1964.

[20] T.W. Jackson, K.R. Purdy, Resonant pulsating flow and convective heat transfer, J. Heat Transfer 87 (1965) 507–512.

[21] N. Fujita, T. Tsubouchi, An experimental study of unsteady heat transfer from a flat plate to an oscillating air flow, Heat Transfer—Japanese Res. 11 (1982) 31–43.
[22] B. Gebhart, Y. Jaluria, R.L. Mahajan, B. Sammakia, Boundary–Induced Flows and Transport, Taylor and Francis, Washington, DC, 1988.
[23] N.K. Ghaddar, K.Z. Korczak, B.B. Mikic, A.T. Patera, Numerical investigation of incompressible flow in grooved channels, Part 1: Stability and self-sustained oscillations, J. Fluid Mechanics 163 (1986) 99–127.
[24] N.K. Ghaddar, M. Magen, B.B. Mikic, A.T. Patera, Numerical investigation of incompressible flow in grooved channels, Part 2: Oscillatory heat transfer enhancement, J. Fluid Mechanics 168 (1986) 541–567.
[25] M. Greiner, An experimental investigation of resonant heat transfer enhancement in grooved channel, Internat. J. Heat Mass Transfer 34 (1991) 1383–1391.
[26] K. Azar, Enhanced cooling of electric components by flow oscillation, J. Thermophys. Heat Transfer 6 (1992) 700–706.
[27] J.A. Miller, Heat transfer in the oscillating turbulent boundary layer, J. Engrg. Power 91 (1969) 239–244.
[28] F.H. Harlow, E.J. Welch, Numerical calculation of time-dependent viscous incompressible flow of fluid with free surface, Phys. Fluids 8 (1965) 2182–2189.
[29] C.W. Hirt, B.D. Nichols, N.C. Romero, SOLA-A numerical solution algorithm for transient fluid flows, LASL Report, LA-5852, 1975.